CrossMark

ORIGINAL PAPER

Decomposition of governing equations in the analysis of resonant response of a nonlinear and non-ideal vibrating system

**Jan Awrejcewicz · Roman Starosta ·
Grażyna Sypniewska-Kamińska**

Abstract The dynamic response of a nonlinear system with three degrees of freedom in resonance that is loaded, inter alia, with a non-ideal excitation is investigated. A direct current motor (DC motor) with an eccentrically mounted rotor serves as a non-ideal source of energy. The general coordinate corresponding to the rotor dynamics steadily increases as a result of rotational motion. The decomposition of the equations of motion proposed in the paper allows us to separate the vibration of rotor from its rotations. The presented approach can be used to separate the vibration from rotations in many other mechanical and mechatronic systems. The behaviour of the considered non-ideal system near two simultaneously occurring resonances is examined using the Krylov–Bogolyubov averaging method. The stability analysis of the resonant response is also carried out.

Grażyna Sypniewska-Kamińska, Ph.D, research fields: engineering mechanics, nonlinear dynamics.

J. Awrejcewicz
Department of Automatics, Biomechanics and Mechatronics, Łódź University of Technology, 1/15 Stefanowski St, 90-924 Lodz, Poland

J. Awrejcewicz
Department of Vehicles, Warsaw University of Technology, 84 Narbutt St, 02-524 Warsaw, Poland

R. Starosta · G. Sypniewska-Kamińska (✉)
Institute of Applied Mechanics, Poznań University of Technology, Piotrowo 3, 60-965 Poznan, Poland
e-mail: grazyna.sypniewska-kaminska@put.poznan.pl

1 Introduction

In modelling the excitation of vibrating systems, one can distinguish two approaches. The first one assumes that the behaviour of the source of excitation is not influenced by the system being forced. In this case, the excitation may be expressed as a given function of time. Such a source of excitation is called an ideal one. The second approach, which recognizes that the vibrating system also influences the work of the excitation source, is more accurate. In most engineering problems, the motion of vibrating systems affects less or more the behaviour of the source of energy which causes the vibration. A source, which is influenced by the response of the vibrating system, is said to be a non-ideal one. On the other hand, a vibrating system forced by a non-ideal source is called a non-ideal system. When the source of excitation is non-ideal, its dynamic behaviour and the reciprocal interactions between the vibrating system and the source should be taken into account in the mathematical modelling of the problem. Namely, the source becomes part of the whole studied system. In effect, at least one additional equation that describes the motion of the source is required, and moreover, the supplementary feedback appears in the equations of motion. All that causes dynamics of the non-ideal vibrating system requires a more

Springer

sophisticated mathematical description, especially when nonlinearities are also taken into account.

Power supplied to a non-ideal system is generally limited. For this reason, dynamical behaviour of such a system may differ significantly from its ideal counterpart. The limiting of supplied energy becomes especially distinct in resonant conditions. Most often an unbalanced DC electric motor situated on an elastic structure is assumed as a non-ideal excitation source. In the neighbourhood of resonant frequency of the supporting structure, majority of the supplied energy is consumed by vibration of this structure. Therefore, great increase in the vibration amplitude is observed, but the angular velocity of the DC motor increases only slightly, or in other words its increase requires a lot of energy, much more than in non-resonant conditions. Afterwards, upon exceeding certain thresholds, the angular velocity of the rotor suddenly increases, and the amplitude of vibrations of the supporting structure decreases rapidly. When the power supplied to the system is reduced during the passage through the resonance, the jump phenomena are also observed, but the threshold values are not the same as in the case described previously. Such a behaviour, characteristic only in the case of a non-ideal system, is known as the Sommerfeld effect.

There is a large number of works devoted to various aspects of the dynamics of non-ideal systems. A broad overview of investigations in the field of non-ideal vibration was described by Balthazar et al. in [1]. The vast majority of the works involving non-ideal systems concerns the Sommerfeld effect which was discovered in 1902 [2]. In particular, the book [3], entirely devoted to the Sommerfeld effect in linear and nonlinear systems, should be mentioned here. Regular and chaotic vibrations of a non-ideal system with two degrees of freedom operating near internal resonances 1:1 and 1:2 were investigated in [4] and [5], respectively. All springs and dampers were assumed there as linear elements, and the system was coupled linearly. So, only nonlinear members resulting from the interaction between the vibrating system and the energy source were taken into account. In paper [6], dynamics of a cantilever beam, modelled by the non-ideal Duffing–Rayleigh oscillator, is investigated in a broad aspect. The authors present and discuss non-stationary and steady-state responses of the system in the resonance region as well as its passage through resonance based on the analytical and numerical approach. The

Sommerfeld effect in rotor dynamics and the influence of external and internal damping on the Sommerfeld effect are the subject of the works [7,8]. Papers [9] and [10] deal with the resonant response of a modified variant of the van der Pol–Mathieu oscillator with nonlinear spring and parametric excitation which is disturbed by a non-ideal source. In [9] is also presented a chaotic aspect of vibration of such an oscillator. Some results of numerical simulations concerning mainly energy transfer and chaotic behaviour of the non-ideal system with one or two pendulums attached to the support are presented in [11] and [12], respectively. The motion of the non-ideal system at the resonance is exposed to the loss of stability; therefore, many investigations are focused on the problem of passage of the system through the resonance as well as control of this passage. An optimal law of control of the DC motor ensuring that a two-degree of freedom system passes through the first resonant peak with the minimum amplitude of the main mass is proposed in [13]. Paper [14] presents a control strategy which was applied to two nonlinear systems with two degrees of freedom: ideal and non-ideal one in order to suppress chaotic oscillations and to improve the transient response of the systems. The results concerning attenuation or elimination of the Sommerfeld effect with the help of appropriately chosen magnetorheological dampers were described in [15].

In all previously mentioned papers, the driving torque of the source of energy (i.e. DC motor) was assumed as a linear function of the angular velocity. In paper [16], where some dynamical features of the Duffing oscillator are investigated, the non-ideal source is assumed as an alternative voltage source harmonically variable in time.

In most papers, the analytical approach devoted to non-ideal systems is based on the application of the Bogolyubov–Krylov averaging method or its modified versions [9,16]. However, recently in several papers the multiple-scale method in time has been adopted to investigate the resonance behaviour of 1-dof system [17,18].

For certain parameters, the chaotic motion can appear in the non-ideal system. Such problems have been discussed in paper [19]. The Pyragas method is applied there to control chaotic motion.

A new approach to study the non-ideal system, including special decomposition of equations and yielding the equation which describes vibration of the rotor, has been presented in [20]. This approach is in
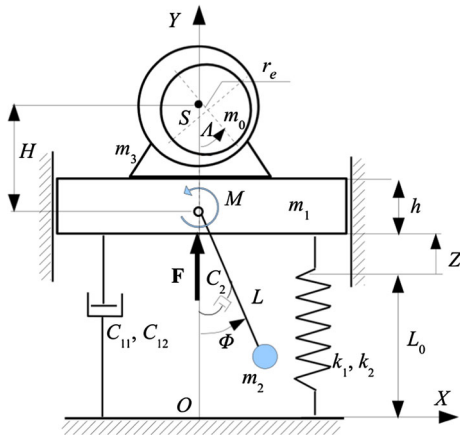
Fig. 1 The investigated system

a certain sense similar to the commonly used method consisting in the subtraction of the increase of the angle caused by pure rotation from the results obtained experimentally or numerically, which describe both the vibration and the effect of the rotation.

The decomposition into the rotations and the oscillations proposed in [20] and developed in the present paper refers to the model equations. The procedure, carried out in such a way, leads to the model equations containing the unknown functions, which describe only the vibration of the whole system. Such a form of equations allows us to apply the Krylov–Bogolyubov averaging method in order to investigate the behaviour of the non-ideal system in the resonance case. This is the main novelty of the approach presented in the paper.

However, the proposed method applies to a particular system. The form of the separated equation depends on the characteristics of the excitation source. The decomposition presented in this paper does not have any common links with the approach consisting in the decomposition of the motion into the slow and fast components, which is widely discussed in works of Blekhman [21]. It is worth to emphasize that the equations describing only vibration of the system have been obtained by introducing the exact solution into the original equations, unlike the general approach presented in [21], where the equations have been derived with the help of the averaging procedures.

The system investigated in the paper is shown in Fig. 1. The electric DC motor with the eccentrically mounted rotor is assumed to be a non-ideal source of vibrations. In this case, the additional degree of free-

dom appears and it is related to the motion of the rotor. Since the generalized coordinate describing the rotor motion grows infinitely in time, the whole process cannot be considered as vibrational. In order to avoid this difficulty, we applied the decomposition of the equation of motion related to the rotor and separation of rotations and vibration. As a result of the decomposition, a new set of equations of motion is derived, where all generalized coordinates describe only the vibration.

2 Formulation of the problem

Let us consider planar motion of the system composed of the support of mass m_1 which can move vertically, the mathematical pendulum of mass m_2 and length L, and the DC motor as the non-ideal source of energy. The studied system is presented in Fig. 1. It is assumed that the stator of the motor whose mass is equal to m_3 does not move with respect to the support. The rotor of mass m_0 is eccentrically installed on the axis of rotation passing through point S. The mass centre of the rotor lies at the crossing point of the axes of symmetry shown in Fig. 1 as two perpendicular dashed lines. Eccentricity of the rotor is denoted by r_e. I_0 is the moment of inertia of the rotor about its central axis. The pendulum is attached to the support by a joint. The support, in turn, is connected to the basis via a viscous damped elastic suspension. Both the spring and the damper are assumed as nonlinear. The elasticity of cubic type has been taken into account, where k_1 and k_2 are the linear and nonlinear elastic coefficients, respectively. The Rayleigh damping model is admitted, whereas damping coefficients are denoted by C_{11} and C_{12}. The length of the non-stretched spring equals L_0. The coefficient denoted by C_2 is associated with viscous damping at the joint connecting the pendulum with the support. The known force F acting vertically on the support and the torque M loading the pendulum change harmonically in the following way: $F = F_0 \cos(\Omega_1 t)$ and $M = M_0 \cos(\Omega_2 t)$. In accordance with the commonly used characteristics of DC motors, the produced torque M_p depends linearly on angular velocity. Therefore, $M_p = U_1 - U_2 \dot{\Lambda}(t)$, where U_1 and U_2 are the constants depending on the electromagnetic field and some geometric features of the DC motor. Angular velocity $\dot{\Lambda}(t)$ oscillates as a result of the rotor unbalancing as well as interaction with the support. Variation of the

angular velocity causes that torque M_p is not constant even during stationary operation.

The system has three degrees of freedom owing to the reciprocal interactions between the support and the source of excitation. Total spring elongation $Z(t)$ and angles $\Phi(t)$ and $\Lambda(t)$ are chosen as generalized coordinates of the system. Kinetic energy relative to the motionless frame and written in the Cartesian coordinate system OXY reads

$$
\begin{aligned}
T = & \frac{1}{2}m_1\left(\dot{X}_1^2 + \dot{Y}_1^2\right) + \frac{1}{2}m_2\left(\dot{X}_2^2 + \dot{Y}_2^2\right) \\
& + \frac{1}{2}m_3\left(\dot{X}_3^2 + \dot{Y}_3^2\right) + \frac{1}{2}m_0\left(\dot{X}_0^2 + \dot{Y}_0^2\right) \\
& + \frac{1}{2}I_0\dot{\Lambda}^2,
\end{aligned}
\tag{1}
$$

where $X_1 = 0$, $Y_1(t) = L_0 + Z(t) + h/2$ are the coordinates of the movable support, $X_3 = 0$, $Y_3 = Y_1 + H$ are the coordinates of the stator mass centre, $X_2 = L\sin(\Phi(t))$, $Y_2 = Y_1 - L\cos(\Phi(t))$ are the coordinates of the suspended pendulum, and $X_0 = r_e\sin(\Lambda(t))$, $Y_0 = Y_1 + H - r_e\cos(\Lambda(t))$ are the coordinates of the mass centre of the eccentrically mounted rotor, whereas g is the gravity of Earth.

All conservative forces which act in the system are yielded by the potential energy

$$
\begin{aligned}
V = & m_0 g Y_0 + m_2 g Y_1 + m_1 g Y_2 + m_3 g Y_3 \\
& + \frac{1}{2}k_1 Z^2 + \frac{1}{4}k_2 Z^4.
\end{aligned}
\tag{2}
$$

The position of stable equilibrium of the system is determined by values Z_e, Φ_e, Λ_e of the generalized coordinates which satisfy the following relations

$$
k_1 Z_e + k_2 Z_e^3 = -m_c g, \quad \Phi_e = 0, \quad \Lambda_e = 0,
\tag{3}
$$

where $m_c = m_0 + m_1 + m_2 + m_3$ is the total mass of the system.

The non-conservative forces acting on the system are introduced as generalized forces. The equations of motion around the equilibrium position have been obtained using Lagrange equations of the second kind and they are as follows

$$
\begin{aligned}
& m_c\ddot{Z}_1 + k_1 Z_1 + 3k_2 Z_e^2 Z_1 + 3k_2 Z_e Z_1^2 + k_2 Z_1^3 \\
& \quad + C_{11}\dot{Z}_1 + C_{12}\dot{Z}_1^3 + m_0 r_e\dot{\Lambda}^2\cos\Lambda \\
& \quad + Lm_1\dot{\Phi}^2\cos\Phi + m_0 r_e\ddot{\Lambda}\sin\Lambda - Lm_1\ddot{\Phi}\sin\Phi \\
& \quad - F_0\cos(\Omega_1 t) = 0,
\end{aligned}
\tag{4}
$$

$$
\begin{aligned}
& L^2 m_2\ddot{\Phi} + Lgm_2\sin\Phi + C_2\dot{\Phi} + Lm_2\ddot{Z}_1\sin\Phi \\
& \quad - M_0\cos(\Omega_2 t) = 0,
\end{aligned}
\tag{5}
$$

$$
\begin{aligned}
& \left(I_0 + m_0 r_e^2\right)\ddot{\Lambda} + gm_0 r_e\sin\Lambda - U_1 + U_2\dot{\Lambda} \\
& \quad + m_0 r_e\ddot{Z}_1\sin\Lambda = 0,
\end{aligned}
\tag{6}
$$

where $Z_1 = Z - Z_e$ is the dynamic elongation of the spring (measured from the equilibrium position). Characteristic frequencies associated with coordinates $Z(t)$, $\Phi(t)$ and $\Lambda(t)$ are: $\omega_1 = \sqrt{k_1/m_c}$, $\omega_2 = \sqrt{g/L}$, $\omega_3 = \sqrt{gm_0 r_e/I_0}$.

Let us introduce dimensionless time $\tau = t\omega_1$ and dimensionless coordinate $\tilde{z} = Z_1/\delta$, where $\delta = m_c g/k_1 = g/\omega_1^2$ is the static elongation of the linear spring of elastic constant equal to k_1. Moreover, the following dimensionless parameters are defined: eccentricity $\beta_e = r_e/L$, mass fractions $\mu_2 = m_2/m_c$ and $\mu_0 = m_0/m_c$; frequencies $w_2 = \omega_2/\omega_1$, $w_3 = \omega_3/\omega_1$, $p_1 = \Omega_1/\omega_1$, $p_2 = \Omega_2/\omega_1$; amplitudes of the external excitations $f_1 = F_0/Lm_c\omega_1^2$, $f_2 = M_0/L^2 m_2\omega_1^2$; parameters of the DC motor characteristics $u_1 = U_1/I_0\omega_1^2$, $u_2 = U_2/I_0\omega_1$; damping coefficients $c_{11} = C_{11}/m_c\omega_1$, $c_{12} = C_{12}\delta^2\omega_1/m_c$, $c_2 = C_2/L^2 m_2\omega_1$; nonlinear stiffness coefficient $\gamma = \frac{k_1}{k_2}\delta$; nonlinear value $z_e = Z_e/\delta$ corresponding to the extension of the spring at equilibrium position.

The following equation has to be fulfilled in the equilibrium position $z_e + \gamma z_e^3 = -1$. The above equation is the dimensionless counterpart of relations (3) and allows us to express nonlinear part of stiffness γ of the spring by static elongation $\gamma = -(1 + z_e)z_e^{-3}$.

In this way, nonlinear properties of the spring may be expressed by static elongation z_e. After introducing all of the above dimensionless quantities, the equations of motion take the following form
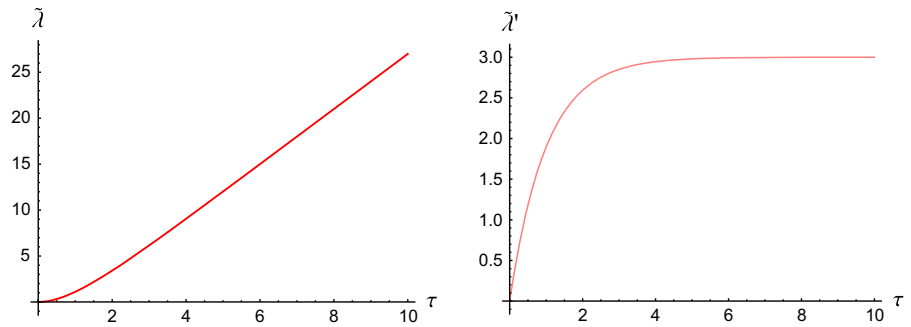
$$
\begin{aligned}
& \ddot{\tilde{z}} + \tilde{z} - \frac{3(1 + z_e)}{z_e}\tilde{z} - \frac{3(1 + z_e)}{z_e^2}\tilde{z}^2 - \frac{(1 + z_e)}{z_e^3}\tilde{z}^3 \\
& \quad + c_{11}\dot{\tilde{z}} + c_{12}\dot{\tilde{z}}^3 + \beta_e\mu_0\dot{\tilde{\lambda}}^2\cos\tilde{\lambda} + \frac{\mu_2}{w_2^2}\dot{\tilde{\varphi}}^2\cos\tilde{\varphi} \\
& \quad + \beta_e\mu_0\ddot{\tilde{\lambda}}\sin\tilde{\lambda} + \frac{\mu_2}{w_2^2}\ddot{\tilde{\varphi}}\sin\tilde{\varphi} - f_1\cos(p_1\tau) = 0,
\end{aligned}
\tag{7}
$$

$$
\ddot{\tilde{\varphi}} + w_2^2\sin\tilde{\varphi}\left(1 + \ddot{\tilde{z}}\right) + c_2\dot{\tilde{\varphi}} - f_2\cos(p_2\tau) = 0,
\tag{8}
$$

$$
\left(1 + w_3^2\beta_e\right)\ddot{\tilde{\lambda}} + w_3^2\sin\tilde{\lambda}\left(1 + \ddot{\tilde{z}}\right) - u_1 + u_2\dot{\tilde{\lambda}} = 0.
\tag{9}
$$

Now, functions denoted by $\tilde{z}$, $\tilde{\varphi}$, $\tilde{\lambda}$ (corresponding to generalized coordinates Z, Φ, Λ) depend on time τ. Equations (7)–(9) are supplemented by the initial

Fig. 2 Time history of $\tilde{\lambda}$ and $\dot{\tilde{\lambda}}$ for SET1

following conditions

$$\tilde{z}(0) = z_0,\ \dot{\tilde{z}}(0) = v_0,\ \tilde{\varphi}(0) = \varphi_0,\ \dot{\tilde{\varphi}}(0) = \omega_{0\varphi},$$
$$\tilde{\lambda}(0) = \lambda_0,\ \dot{\tilde{\lambda}}(0) = \omega_{0\lambda},$$

where $z_0, v_0, \varphi_0, \omega_{0\varphi}, \lambda_0, \omega_{0\lambda}$ are known.

3 Decomposition of the governing equations

Coordinate $\tilde{\lambda}(\tau)$ is equal to the angle measured from the initial position. After each rotation of the rotor, the angle increases by 2π. This increase is dominant in time history of $\tilde{\lambda}(\tau)$ which is shown in Fig. 2. This graph and several subsequent graphs are made for the chosen data included in the set

$$\text{SET1} = \{f_1 = 0.0085,\ f_2 = 0.003,\ p_1 = 0.2,$$
$$p_2 = 0.4,\ c_{11} = 0.0008,\ c_{12} = 0.000008,$$
$$c_2 = 0.0001,\ \beta_e = 0.05,\ \mu_1 = 1/6,$$
$$\mu_0 = 1/15,\ u_1 = 3.,\ u_2 = 1,\ w_2 = 0.045,$$
$$w_3 = 0.016,\ z_e = -0.99,\ z_0 = 0,\ v_0 = 0,$$
$$\varphi_0 = 0.1,\ \omega_{0\varphi} = 0,\ \lambda_0 = 0,\ \omega_{0\lambda} = 0\}.$$

However, in the time history of $\tilde{\lambda}(\tau)$, there are also oscillations caused by the rotor unbalance and influence of the vibration of the support. Oscillations of the rotor play a significant role in dynamics of the whole system. In order to study the interactions between particular parts of the system, for instance near resonance, these oscillations should be separated from the rotational motion.

Thus, it is desirable to split function $\tilde{\lambda}(\tau)$ into a component describing the unlimited increase and the second one relative to pure oscillations. We propose decomposition of this function in the following manner:

$$\tilde{\lambda}(\tau) = \alpha_0(\tau) + \alpha_1(\tau), \tag{10}$$

where function $\alpha_0(\tau)$ satisfies the initial value problem of the linear differential equation and inhomogeneous initial conditions

$$\left(1 + w_3^2 \beta_e\right) \ddot{\alpha}_0 - u_1 + u_2 \dot{\alpha}_0 = 0,$$
$$\alpha_0(0) = \lambda_0,\ \dot{\alpha}_0(0) = \omega_{0\lambda}. \tag{11}$$

The Cauchy problem (11) describes dynamics of the rotation of the rotor under the action of linearly changing torque and can be solved analytically.

Substituting the assumption given by (10) and differential equation $(11)_1$ into Eqs. (7)–(9), we obtain a new form of the governing equations with unknown functions denoted by z, ϕ and α_1

$$\ddot{z} + z - \frac{3(1+z_e)}{z_e}z - \frac{3(1+z_e)}{z_e^2}z^2 - \frac{(1+z_e)}{z_e^3}z^3$$
$$+ c_{11}\dot{z} + c_{12}\dot{z}^3 + \beta_e\mu_0\left(\dot{\alpha}_0 + \dot{\alpha}_1\right)^2 \cos\left(\alpha_0 + \alpha_1\right)$$
$$+ \frac{\mu_1}{w_2^2}\dot{\varphi}^2 \cos\varphi + \beta_e\mu_0\left(\ddot{\alpha}_0 + \ddot{\alpha}_1\right) \sin\left(\alpha_0 + \alpha_1\right)$$
$$+ \frac{\mu_2}{w_2^2}\ddot{\varphi} \sin\varphi - f_1\cos\left(p_1\tau\right) = 0 \tag{12}$$

$$\ddot{\varphi} + w_2^2 \sin\varphi + c_2\dot{\varphi} + w_2^2\ddot{z} \sin\varphi - f_2\cos\left(p_2\tau\right) = 0, \tag{13}$$

$$\left(1 + w_3^2\beta_e\right)\ddot{\alpha}_1 + w_3^2 \sin\left(\alpha_0 + \alpha_1\right) + u_2\dot{\alpha}_1$$
$$+ w_3^2\ddot{z} \sin\left(\alpha_0 + \alpha_1\right) = 0. \tag{14}$$

The initial conditions supplementary to set (12)–(14) are as follows

$$z(0) = z_0,\ \dot{z}(0) = v_0,\ \varphi(0) = \varphi_0,\ \dot{\varphi}(0) = \omega_{0\varphi},$$
$$\alpha_1(0) = 0,\ \dot{\alpha}_1(0) = 0.$$

Taking into account the proposition (10), the original initial value problem (7)–(9) is transformed into two problems, i.e. the problem of pure rotation of the rotor given by (11), and the problem of pure oscillations of the whole system described by (12)–(14) with their
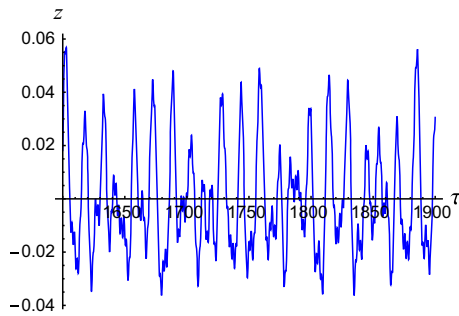
Fig. 3 Time history of z for data from SET1

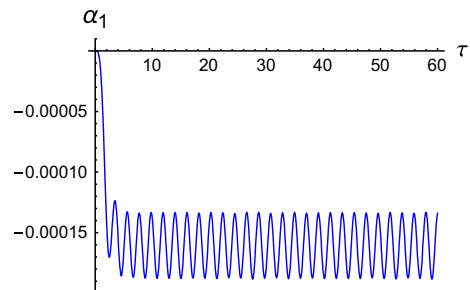**Fig. 4** Time history of φ for data from SET1
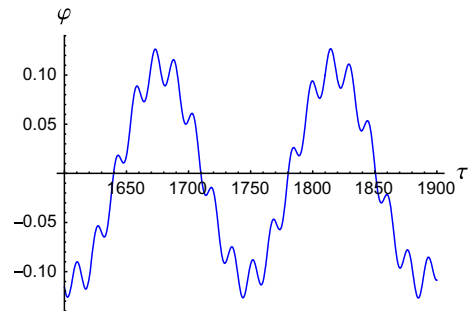
Fig. 5 Time history of α_1 for data from SET1

initial conditions. In the first case, the term "pure" is used to emphasize that rotation $\alpha_0(\tau)$ does not depend on the rotor unbalancing or interactions between parts of the system. In the second case, it is used to note that the oscillations have been completely separated from the rotations. Let us note that in Eqs. (12)–(14), function $\alpha_0(\tau)$ is a solution of problem (11) and it has the following form

$$
\alpha_0 = -\frac{u_1}{u_2^2} + \frac{\omega_{0\lambda}}{u_2}
$$
$$
+ \frac{(u_1 - u_2\omega_{0\lambda})\left(1 + w_3^2\beta_e\right)\exp\left(-\frac{u_2\tau}{1+w_3^2\beta_e}\right)}{u_2^2}
$$
$$
- \frac{(u_1 - u_2\omega_{0\lambda})\,w_3\beta_e}{u_2^2} + \lambda_0 + \frac{u_1\tau}{u_2}. \tag{15}
$$

It should be noticed that function $\alpha_1(\tau)$ describes oscillations of the rotor around its rotation expressed by function $\alpha_0(\tau)$. In Eqs. (12) and (14), some trigonometric functions appear with argument in the form of sum $\alpha_0(\tau) + \alpha_1(\tau)$. Afterwards, we expand them using the classical trigonometric identities. Consequently, the coefficients in differential equations (12) and (14) are the functions of time τ.

Equations (12)–(14), yielded by the proposed decomposition of the original problem, describe pure oscillations of the system. Time histories of z, φ and α_1 obtained as solutions of the initial problem given by (12)–(14) and supplementary initial conditions are presented in Figs. 3, 4 and 5.

Coincidence of the solutions of original initial problem (7)–(9) and problem (12)–(14) together with the solution (15) is confirmed based on the results presented in Fig. 6 which validates our decomposition proposal. The following differences are presented on

the vertical axes: $\Delta_z = \tilde{z} - z$, $\Delta_\varphi = \tilde{\varphi} - \varphi$, $\Delta_\alpha = \tilde{\lambda} - (\alpha_0 + \alpha_1)$.

Very high conformity of solutions of both initial problems has been achieved numerically for many various parameters despite the fact that assumption (10) does not lead to the general solution of problem (7)–(9).

Function $\alpha_1(\tau)$ describes, in principle, oscillations of the non-ideal source (beyond the transitional period). Time histories of derivative $\dot{\alpha}_0(\tau)$ and the sum of derivatives $\dot{\alpha}_0(\tau) + \dot{\alpha}_1(\tau)$ are shown in Fig. 7. It is clearly visible in this figure that time derivative of $\alpha_1(\tau)$ oscillates around angular velocity of the stationary rotational motion.

Function $\alpha_0(\tau)$ given by expression (15) is presented graphically in Fig. 8 for data included in SET1. Let us observe that when time τ tends to infinity, function $\alpha_0(\tau)$ approaches its asymptote

$$
\lim_{\tau\to\infty}(\alpha_0(\tau)) = -\frac{u_1}{u_2^2} + \frac{\omega_{0\lambda}}{u_2} + \frac{(u_2\omega_{0\lambda} - u_1)\,w_3^2\beta_e}{u_2^2}
$$
$$
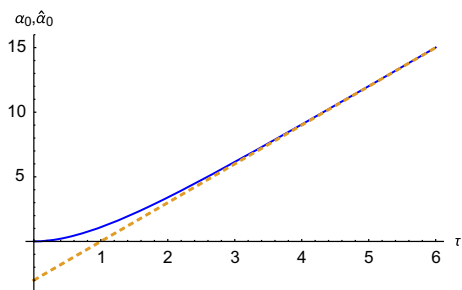+ \lambda_0 + \frac{u_1\tau}{u_2} = \hat{\alpha}_0(\tau). \tag{16}
$$

Therefore, exponential transient component $\exp\left(-\frac{u_2\tau}{1+w_3^2\beta_e}\right)$, which disappears in time, can be omitted, apart from the initial stage of motion. Owing
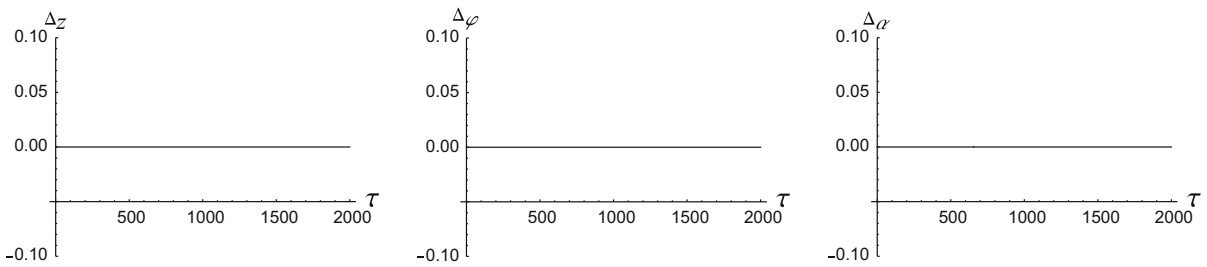
Fig. 6 Identity of solutions: $\tilde{z}$ versus z, $\tilde{\varphi}$ versus φ and $\tilde{\lambda}$ versus $(\alpha_0 + \alpha_1)$ for data from SET1
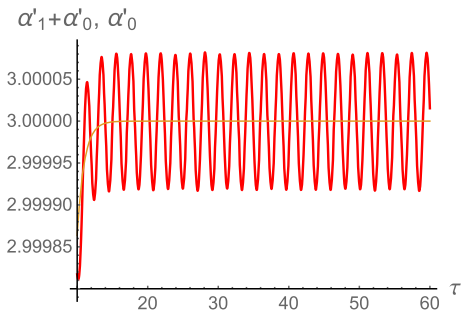
Fig. 7 Time histories of $\dot{\alpha}_0$ and $(\dot{\alpha}_0 + \dot{\alpha}_1)$ for data from SET1

Fig. 8 Asymptotic convergence of α_0 and $\hat{\alpha}_0$ for data from SET1

to this observation, we can approximate solution (15) in the following manner

$$\alpha_0\,(\tau) \approx \hat{\alpha}_0\,(\tau). \tag{17}$$

In order to validate approximation (17), we compare the solutions of equations (12)–(14) obtained using function $\alpha_0\,(\tau)$ given by (15) (i.e. the exact solution of (11)) with the solutions of the same set of equations into which approximate function $\hat{\alpha}_0\,(\tau)$ is introduced. Results of the comparison are shown in Fig. 9. Coordinates on the vertical axes are marked by z, φ, α_1 or $\hat{z}$, $\hat{\varphi}$, $\hat{\alpha}_1$ when the exact or approximate solution of (11) is used, respectively.

We can observe that omitting of the transient component causes a rather negligible change in time histories

of coordinates $z\,(\tau)$ and $\varphi\,(\tau)$. The difference between solutions $\alpha_1(\tau)$ and $\hat{\alpha}_1(\tau)$ consists only in shifting one to another which is caused by the impact of the transient effects. We can observe in Fig. 10, where these solutions are drawn in much shorter time interval, that their amplitudes, periods and phases are the same.

Therefore, in the steady state we can introduce assumption (17) into Eqs. (12)–(14). In this way, we have the following set of the approximate equations of motion

$$\ddot{\hat{z}} + \hat{z} - \frac{3\,(1 + z_e)}{z_e}\hat{z} - \frac{3\,(1 + z_e)}{z_e^2}\hat{z}^2$$
$$- \frac{3\,(1 + z_e)}{z_e^3}\hat{z}^3 + c_{11}\dot{\hat{z}} + c_{12}\dot{\hat{z}}^3 + \beta_e\mu_0\left(\dot{\hat{\alpha}}_0 + \dot{\hat{\alpha}}_1\right)^2$$
$$\times \left(\cos\hat{\alpha}_0\cos\hat{\alpha}_1 - \sin\hat{\alpha}_0\sin\hat{\alpha}_1\right) + \frac{\mu_1}{w_2^2}\dot{\hat{\varphi}}^2\cos\hat{\varphi}$$
$$\times \beta_e\mu_0\left(\ddot{\hat{\alpha}}_0 + \ddot{\hat{\alpha}}_1\right)\left(\sin\hat{\alpha}_0\cos\hat{\alpha}_1 + \cos\hat{\alpha}_0\sin\hat{\alpha}_1\right)$$
$$+ \frac{\mu_2}{w_2^2}\ddot{\hat{\varphi}}\sin\hat{\varphi} - f_1\cos\left(p_1\tau\right) = 0 \tag{18}$$

$$\ddot{\hat{\varphi}} + w_2^2\sin\hat{\varphi} + c_2\dot{\hat{\varphi}} + \ddot{\hat{z}}\sin\hat{\varphi} - f_2\cos\left(p_2\tau\right) = 0, \tag{19}$$

$$\left(1 + w_3^2\beta_e\right)\ddot{\hat{\alpha}}_1 + w_3^2\left(1 + \ddot{\hat{z}}\right)$$
$$\times \left(\sin\hat{\alpha}_0\cos\hat{\alpha}_1 + \cos\hat{\alpha}_0\sin\hat{\alpha}_1\right) + u_2\dot{\hat{\alpha}}_1 = 0. \tag{20}$$

Due to approximation (17), the time-dependent coefficients in equations (18) and (20) are periodic with the period equal to $2\pi u_2/u_1$. Therefore, the steady-state behaviour of the system is described by the equations of the Hill type.
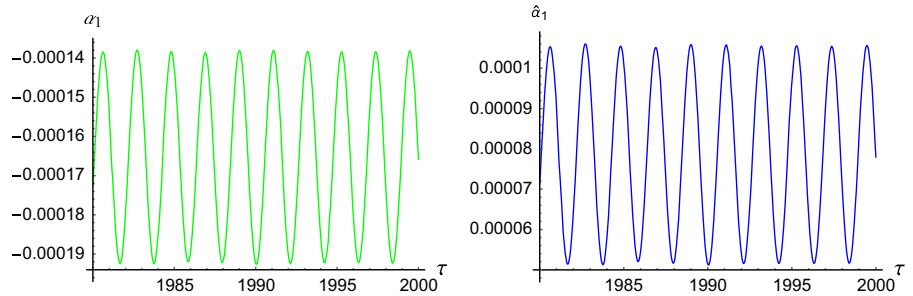
4 Vibration near resonance

Two simultaneously occurring resonances are considered, i.e. the main external resonance $p_1 = 1$ and the parametric one $u_1/u_2 = 2$, related to the interactions
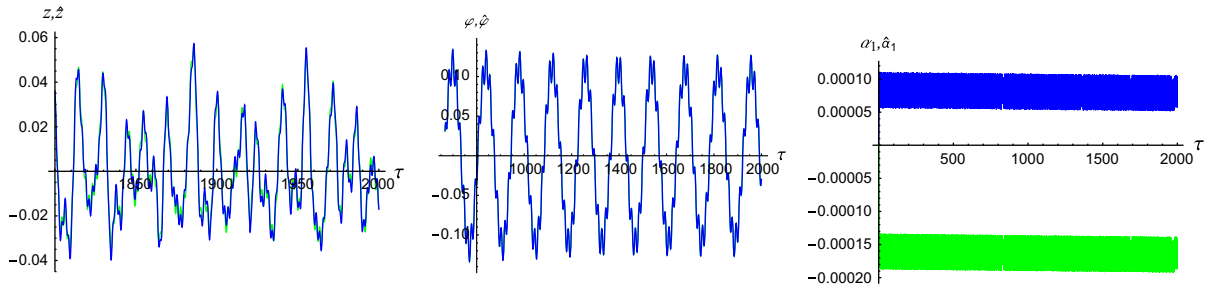
Fig. 9 Comparison of solutions of the problem (12)–(14) obtained for α_0 and $\hat{\alpha}_0$; data from SET1

Fig. 10 Comparison of time histories $\alpha_1(\tau)$ and $\hat{\alpha}_1(\tau)$; data from SET1

between the support and the unbalanced rotor. In paper [19], the second one was detected as dominant by the Fourier analysis for a similar non-ideal system. In order to investigate the resonant state, we apply the averaging method similar to the one presented in [9,10].

Firstly, we approximate the geometric nonlinearities by polynomial ones, expanding trigonometric functions in Eqs. (18)–(20) in the Taylor series

$$\sin\left(\hat{\varphi}\right) \approx \hat{\varphi} - \frac{\hat{\varphi}^3}{6}, \ \cos\left(\hat{\varphi}\right) \approx 1 - \frac{\hat{\varphi}^2}{2}, \ \sin\left(\hat{\alpha}_1\right)$$
$$\approx \hat{\alpha}_1 - \frac{\hat{\alpha}_1^3}{6}, \ \cos\left(\hat{\alpha}_1\right) \approx 1 - \frac{\hat{\alpha}_1^2}{2}. \quad (21)$$

Next, in order to simplify the notation, we introduce the new variable τ_1 related to dimensionless time τ as follows:

$$-\frac{u_1}{u_2^2} + \frac{\omega_{0\lambda}}{u_2} + \frac{(u_2\omega_{0\lambda} - u_1)\,w_3^2\beta_e}{u_2^2}$$
$$+ \lambda_0 + \frac{u_1\tau}{u_2} = \frac{u_1\tau_1}{u_2}. \quad (22)$$

Taking advantage of approximations (21) and introducing shifted time τ_1 into Eqs. (18)–(20), we obtain the following new form of the equations of motion

$$-f_1\cos\left(p_1\xi\right)\cos\left(p_1\tau_1\right) + f_1\sin\left(p_1\xi\right)\sin\left(p_1\tau_1\right)$$
$$+ \ddot{\hat{z}} + \hat{z} - \frac{1 + z_e}{z_e^3}\left(3z_e^2\hat{z} + 3z_e\hat{z}^2 + \hat{z}^3\right) + c_{11}\dot{\hat{z}}$$

$$+ c_{12}\dot{\hat{z}}^3 + \frac{\mu_1\dot{\hat{\varphi}}^2}{w_2^2} - \frac{\mu_1\hat{\varphi}^2\dot{\hat{\varphi}}^2}{2w_2^2} + \beta_e\mu_0\sin\left(u\tau_1\right)\ddot{\hat{\alpha}}_1$$
$$+ \frac{\mu_1\hat{\varphi}\ddot{\hat{\varphi}}}{w_2^2}\left(1 - \frac{\hat{\varphi}^2}{6}\right)\left(1 - \frac{\hat{\alpha}_1^2}{2}\right)\left(\beta_e\mu_0\cos\left(u\tau_1\right)\right.$$
$$\times\left(u^2 + 2u\dot{\hat{\alpha}}_1 + \dot{\hat{\alpha}}_1^2\right) + \beta_e\mu_0\sin\left(u\tau_1\right)\ddot{\hat{\alpha}}_1\right)$$
$$\times\left(\frac{\hat{\alpha}_1^3}{6} - \hat{\alpha}_1\right)\left(\beta_e\mu_0\sin\left(u\tau_1\right)\left(u^2 + 2u\dot{\hat{\alpha}}_1 + \dot{\hat{\alpha}}_1^2\right)\right.$$
$$\left. - \beta_e\mu_0\cos\left(u\tau_1\right)\ddot{\hat{\alpha}}_1\right) = 0 \quad (23)$$
$$-f_2\left(\cos\left(p_2\xi\right)\cos\left(p_2\tau_1\right) - \sin\left(p_2\xi\right)\sin\left(p_2\tau_1\right)\right)$$
$$+ \ddot{\hat{\varphi}} + w_2^2\hat{\varphi} - \frac{w_2^2}{6}\hat{\varphi}^3\left(1 + \ddot{\hat{z}}\right) + c_2\dot{\hat{\varphi}} + w_2^2\hat{\varphi}\hat{z} = 0 \quad (24)$$

$$\ddot{\hat{\alpha}}_1\left(1 + w_3^2\beta_e\right) + \left(1 - \frac{\hat{\alpha}_1^2}{6}\right)w_3^2\hat{\alpha}_1\cos\left(u\tau_1\right)\left(1 + \ddot{\hat{z}}\right)$$
$$+ u_2\dot{\hat{\alpha}}_1 + \left(1 - \frac{\hat{\alpha}_1^2}{2}\right)w_3^2\sin\left(u\tau_1\right)\left(1 + \ddot{\hat{z}}\right) = 0, \quad (25)$$

where $\xi = \frac{1 + w_3^2\beta_e}{u_2} - \frac{u_2\lambda_0 + \lambda_1 + w_3^2\beta_e\lambda_1}{u_1}$.

The most important mechanical effect in the considered problem is the vibration of the support, described by coordinate $\hat{z}(\tau_1)$. Therefore, our further analysis is focused on the resonant behaviour of the support. Func-

tion $\hat{z}(\tau_1)$ is anticipated in the form (see also [9,10])

$$z(\tau_1) = B_1(\tau_1)\cos(\upsilon\tau_1) + B_2(\tau_1)\sin(\upsilon\tau_1), \quad (26)$$

where υ is the multiplicative measure of the "distance" of the frequency from the resonant frequency. The system is in resonance when $\upsilon \to 1$. $B_1(\tau)$ and $B_2(\tau)$ in (26) are the unknown functions describing the modulation of amplitude B and phase Ψ of the support according to

$$B(\tau_1) = \sqrt{B_1^2(\tau_1) + B_2^2(\tau_1)}, \ \Psi(\tau_1)$$
$$= \arctan\left(\frac{B_1(\tau_1)}{B_2(\tau_1)}\right). \quad (27)$$

After introducing (26) into set (23)–(25) and eliminating the secular terms, the modulation equations can be derived in the form

$$-f_1\cos(p_1\xi) + B_1 - 3\frac{1+z_e}{z_e^3}B_1$$
$$\times\left(z_e^2 + \frac{1}{4}B_2^2 + \frac{1}{4}B_1^2\right) - \upsilon^2 B_1 + c_{11}\upsilon B_2$$
$$+\frac{3}{4}c_{12}\upsilon^3 B_2\left(B_1^2 + B_2^2\right) + c_{11}\dot{B}_1 + \frac{3}{2}c_{12}\upsilon^2$$
$$\times\left(\frac{1}{2}B_1^2\dot{B}_1 + \frac{3}{2}B_2^2\dot{B}_1 - B_1 B_2\dot{B}_2\right) + \frac{3}{4}c_{12}\dot{B}_1^3$$
$$+2\upsilon\dot{B}_2 = 0, \quad (28)$$

$$f_1\sin(p_1\xi) - c_{11}\upsilon B_1 - \frac{3}{4}c_{12}\upsilon^3 B_1\left(B_1^2 + B_2^2\right)$$
$$+B_2 - 3\frac{1+z_e}{z_e^3}B_2\left(z_e^2 + \frac{1}{4}B_2^2 + \frac{1}{4}B_1^2\right) - \upsilon^2 B_2$$
$$-2\upsilon\dot{B}_1 + c_{11}\dot{B}_2 + \frac{3}{2}c_{12}\upsilon^2\left(-B_1 B_2\dot{B}_1\right.$$
$$\left.+\frac{3}{2}B_1^2\dot{B}_2 + \frac{1}{2}B_2^2\dot{B}_2\right) + \frac{3}{4}c_{12}\dot{B}_2^3 = 0.$$
$$(29)$$

In order to simplify the notation, argument τ_1 of functions $B_1(\tau)$ and $B_2(\tau)$ is omitted.

In the steady state, all derivatives in (24)–(25) should be equal to zero. The implicit, algebraic form of the amplitude–frequency resonant response is as follows:

$$-f_1\cos(p_1\xi) + B_1 - 3\frac{1+z_e}{z_e^3}B_1$$
$$\times\left(z_e^2 + \frac{1}{4}B_2^2 + \frac{1}{4}B_1^2\right) - \upsilon^2 B_1 + c_{11}\upsilon B_2$$
$$+\frac{3}{4}c_{12}\upsilon^3 B_2\left(B_1^2 + B_2^2\right) = 0, \quad (30)$$

$$f_1\sin(p_1\xi) - c_{11}\upsilon B_1 + B_2 - 3\frac{1+z_e}{z_e^3}B_2$$

$$\times\left(z_e^2 + \frac{1}{4}B_2^2 + \frac{1}{4}B_1^2\right) - \upsilon^2 B_2$$
$$-\frac{3}{4}c_{12}\upsilon^3 B_1\left(B_1^2 + B_2^2\right) = 0. \quad (31)$$

Stability analysis

Let us express the functions in (30) and (31) in the following manner

$$B_1(\tau_1) = B_{10}(\tau_1) + B_{11}(\tau_1), \ B_2(\tau_1) = B_{20}(\tau_1)$$
$$+ B_{21}(\tau_1), \quad (32)$$

where $B_{10}(\tau_1)$ and $B_{20}(\tau_1)$ are the fixed points of Eqs. (28)–(29), i.e. they fulfil Eqs. (30)–(31), whereas $B_{11}(\tau_1)$ and $B_{21}(\tau_1)$ are the perturbations considered to be small with respect to $B_{10}(\tau_1)$ and $B_{20}(\tau_1)$, respectively.

After introducing (32) into Eqs. (30)–(31) and taking into account the fact that $B_{10}(\tau_1)$ and $B_{20}(\tau_1)$ fulfil Eqs. (30)–(31), the perturbed equations are obtained. Their linear counterpart forms are as follows:

$$\dot{B}_{11}\left(c_1 + \frac{3}{4}c_{12}\upsilon^2\left(B_{10}^2 + 3B_{20}^2\right)\right)$$
$$+ B_{11}\left(1 - 3\frac{1+z_e}{z_e^3}\left(\frac{3}{4}B_{10}^2 + \frac{1}{4}B_{20}^2 + z_e^2\right)\right.$$
$$\left.- \upsilon^2 + \frac{3}{2}B_{10}B_{20}c_{12}\upsilon^3\right) + \dot{B}_{21}\left(2\upsilon\right.$$
$$\left.- \frac{3}{2}B_{10}B_{20}c_{12}\upsilon^2\right) + B_{21}\left(-\frac{3(1+z_e)}{2z_e^3}B_{10}B_{20}\right.$$
$$\left.+ c_{11}\upsilon + \frac{3}{4}c_{12}\upsilon^3\left(B_{10}^2 + 3B_{20}^2\right)\right) = 0, \quad (33)$$

$$\dot{B}_{21}\left(c_1 + \frac{3}{4}c_{12}\upsilon^2\left(B_{20}^2 + 3B_{10}^2\right)\right)$$
$$+ B_{21}\left(1 - 3\frac{1+z_e}{z_e^3}\left(\frac{3}{4}B_{20}^2 + \frac{1}{4}B_{10}^2 + z_e^2\right)\right.$$
$$\left.- \upsilon^2 - \frac{3}{2}B_{10}B_{20}c_{12}\upsilon^3\right) + \dot{B}_{11}\left(-2\upsilon\right.$$
$$\left.- \frac{3}{2}B_{10}B_{20}c_{12}\upsilon^2\right) - B_{11}\left(\frac{3(1+z_e)}{2z_e^3}B_{10}B_{20}\right.$$
$$\left.+ c_1\upsilon + \frac{3}{4}c_{12}\upsilon^3\left(B_{20}^2 + 3B_{10}^2\right)\right) = 0. \quad (34)$$

Solutions $B_{10}(\tau_1)$ and $B_{20}(\tau_1)$ are stable when all roots of the characteristic equation of the system (33)–(34) have negative real parts.

The amplitude–frequency relations (30)–(31) allow us to draw resonant response curves. Figure 11 shows four graphs constructed for several different values of

Fig. 11 Resonant curves for various nonlinear damping coefficients c_{12}; *black*—stable, *gray*—unstable
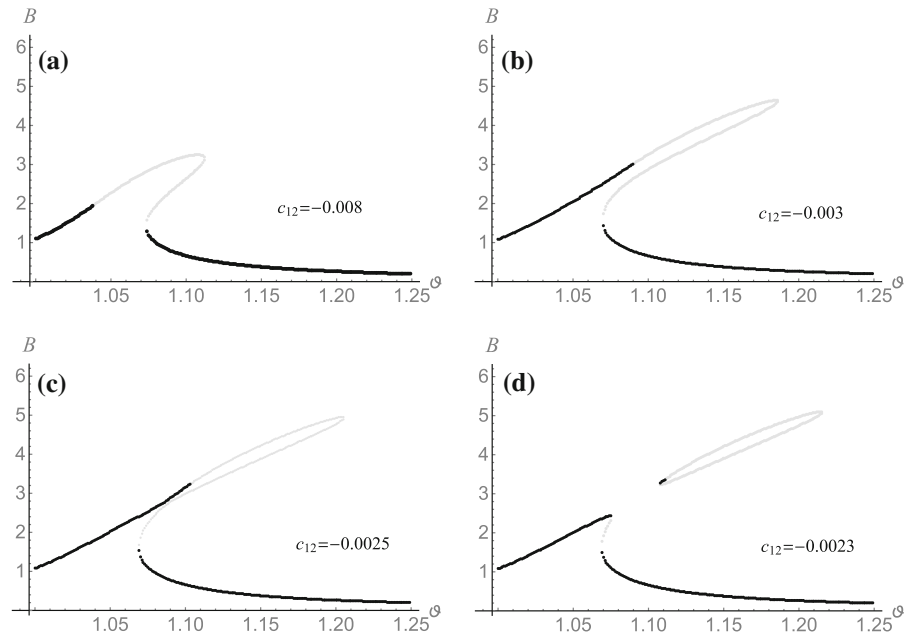
nonlinear damping coefficient c_{12}. All other parameters are the same for each of the included graphs, and their values are collected in SET2, where

$$SET2 = \{f_1 = 0.1, c_{11} = 0.05, c_{12} = 0.008,$$
$$\beta_e = 0.2, u_1 = 4.4, u_2 = 2.2, w_3 = 0.16,$$
$$z_e = -0.98, \lambda_0 = 0, \lambda_1 = 0\}.$$

The dimensionless amplitude B on the vertical axes is related to the value of the linear spring with the elastic constant equal k_1, being loaded by total weight of the system in the equilibrium position.

One can notice that the influence of nonlinearity of damping on the shape of the resonance curves is significant. These few chosen graphs of the amplitude–frequency relation presented in Fig. 11 are representative for the behaviour of the system in the considered resonant conditions. In the cases presented in Fig. 11a and b, the shape of curves is typical of hard springs. However, the analysis of stability reveals dynamic features appropriate only for non-ideal vibrating systems. Upper branch of the resonance curve, which is usually stable in the case of ideal systems, becomes unstable in a certain interval of the frequency. Width of this interval grows with the values of coefficient c_{12}. As a result, there is an interval of υ in which the occurrence of steady-state motion is impossible (see Fig. 11a). This conclusion was confirmed and validated by the direct numerical solution of the governing equations. Namely, when the values of parameter υ are located in the inter-

val corresponding to the loss of stability, all our trials of getting the numerical solutions to the equations of motion were finished due to occurred numerical instability. The shape of resonance response curves presented in Fig. 11c and d differs from the one known from dynamics exhibited by ideal systems. When the values of parameter υ decrease, branches of the curves approach each other (see Fig. 11c) and then the separate branch of the curve appears as it is shown in Fig. 11d. It is worth noting that on the separate branch, there is a stable part. Concluding this issue, one can say that depending on the value of parameter c_{12}, there are two, one or none stable amplitudes for the fixed value of frequency.

5 Conclusions

The nonlinear mechanical system of three degrees of freedom with the non-ideal source of energy has been examined. The unbalanced rotor of DC motor and the external harmonically changing force and torque served as the vibration sources.

The new idea proposed in the present paper consists in the analysis of resonant behaviour of the non-ideal and nonlinear vibrating system based on the decomposition concept. The decomposition of the equations of motion has been proposed in order to separate the infinitely growing coordinate, governing position of the rotor. It should be emphasized that the proposed decomposition procedure is an identity in the mathe-

matical sense. It allows us to examine efficiently the rotor oscillations separately, disregarding its rotations, which essentially simplifies the analysis.

In addition, a detailed study of the case when parametric and primary resonances appear simultaneously has also been performed. The possible amplitudes of the steady-state vibration have been derived analytically and presented graphically. The stability procedure shows that there are some ranges of frequency near resonance where the steady-state motion is impossible. This phenomenon can be connected with the Sommerfeld effect occurring in the non-ideal systems. For some values of parameters, a stable separate loop appears as part of the resonance response curve.

The procedures written in a Mathematica computer algebra system have been used due to high complexity of the symbolic computations.

References

1. Balthazar, J.M., Mook, D.T., Weber, H.I., Brasil, R.M.L.R.F., Fenili, A., Belato, D., Felix, J.L.P.: An overview on non-ideal vibrations. Mecannica **330**(7), 1–9 (2002)
2. Sommerfeld, A.: Beiträge zum dynamischen Ausbau der Festigkeitslehre. Zeitschrift für Physik **3**, 266–286 (1902)
3. Kononenko, V.O.: Vibrating Systems with Limited Power Supply. Iliffe Books, London (1969)
4. Tsuchida, M., de Lolo Guilherme, K., Balthazar, J.M., Silva, G.N., Cheshankov, B.I.: On regular and irregular vibrations of a non-ideal system with two degrees of freedom. 1:1 resonance. J. Sound Vib. **260**(5), 949–960 (2003)
5. Tsuchida, M., de Lolo Guilherme, K., Balthazar, J.M.: On chaotic vibrations of a non-ideal system with two degrees of freedom: 1:2 resonance and Sommerfeld effect. J. Sound Vib. **282**(3–5), 1201–1207 (2005)
6. Felix, J.L.P., Balthazar, J.M., Brasil, R.M.L.R.F.: Comments on nonlinear dynamics of a non-ideal Duffing–Rayleigh oscillator: numerical and analytical approaches. J. Sound Vib. **319**(3–5), 1136–1149 (2009)
7. Samantaray, A.K.: Steady-state dynamics of a non-ideal rotor with internal damping and gyroscopic effects. Nonlinear Dyn. **56**(4), 443–451 (2009)
8. Samantaray, A.K., Dasgupta, S.S., Bhattacharyya, R.: Sommerfeld effect in rotationally symmetric planar dynamical systems. Int. J. Eng. Sci. **48**, 21–36 (2010)
9. Warmiński, J.: Regular and chaotic vibrations of van der Pol–Mathieu oscillator with non-ideal energy source. J. Theor. Appl. Mech. **40**(2), 415–433 (2002)
10. Warmiński, J., Balthazar, J.M., Brasil, R.M.L.R.F.: Vibrations of a non-ideal parametrically and self-excited model. J. Sound Vib. **245**(2), 363–374 (2001)
11. Sado, D., Kot, M.: Chaotic vibration of an autoparametrical system with a non-ideal source of power. J. Theor. Appl. Mech. **45**, 119–131 (2007)
12. Sado, D.: Nonlinear dynamics of a non-ideal autoparametric system with MR damper. Shock Vib. **20**(6), 1065–1072 (2013)
13. Balthazar, J.M., Cheshankov, B.I., Ruschev, D.T., Barbanti, L., Weber, H.I.: Remarks on the passage through resonance of a vibrating system with two degrees of freedom, excited by a non-ideal energy source. J. Sound Vib. **239**(5), 1075–1085 (2001)
14. Tusset, A.M., Balthazar, J.M., Chavarette, F.R., Felix, J.L.P.: On energy transfer phenomena, in a nonlinear ideal and nonideal essential vibrating systems, coupled to a (MR) magneto-rheological damper. Nonlinear Dyn. **69**, 1859–1880 (2012)
15. Piccirillo, V., Tusset, A.M., Balthazar, J.M.: Dynamical jump attenuation in a non-ideal system through a magnetorheological damper. J. Theor. Appl. Mech. **52**(3), 595–604 (2014)
16. Nana Nbendjo, B.R., Caldas, I.L., Viana, R.L.: Dynamical changes from harmonic vibrations of a limited power supply driving a Duffing oscillator. Nonlinear Dyn. **70**, 401–407 (2012)
17. Bolla, M.R., Balthazar, J.M., Felix, J.L.P., Mook, D.T.: On an approximate analytical solution to a nonlinear vibrating problem, excited by a nonideal motor. Nonlinear Dyn. **50**, 841–847 (2007)
18. Alisverisci, G.F., Bayiroglu, H., Ünal, G.: Nonlinear response of vibrational conveyers with non-ideal vibration exciter: primary resonance. Nonlinear Dyn. **69**, 1611–1619 (2013)
19. Zukovic, M., Cveticanin, L.: Chaotic responses in a stable duffing system of non-ideal type. J. Vib. Control **13**(6), 751–767 (2007)
20. Awrejcewicz J., Starosta R., Sypniewska-Kamińska G. Decomposition of the equations of motion in the analysis of dynamics of a 3-DOF nonideal system. Math. Probl. Eng. 8 (2014)
21. Blekhman, I.I.: Vibrational Mechanics: Nonlinear Dynamic Effects, General Approach, Applications. World Scientific, Singapore (1999)